Self-Assembly of Amphiphilic ABC Star Triblock Copolymers and Their Blends with AB Diblock Copolymers in Solution: Self-Consistent Field Theory Simulations

Jian Wai Ma, Xuan Li, Ping Tang,* and Yuliang Yang*

Key Laboratory of Molecular Engineering of Polymer, Ministry of Education, and Department of Macromolecular Science, Fudan University, Shanghai 200433, China

Received: November 17, 2006; In Final Form: December 29, 2006

The self-assembled morphologies of amphiphilic ABC star triblock copolymers consisting of hydrophilic A blocks and hydrophobic B and C blocks and the blends with their counterpart linear AB diblock copolymers in solution are investigated by 2D real-space implementation of self-consistent field theory (SCFT) simulation. The star triblock copolymers self-assemble in solution to form various micellar structures from hamburger, to segmented wormlike, to toroidal segmented micelles, and finally to vesicles with simultaneously increasing hydrophobic lengths of blocks B and C. When the length of hydrophobic blocks B and C is asymmetric, specific bead-on-string worm micelles are found. Particularly, when the star ABC triblock copolymer is in a strong segregation regime and both B and C blocks are strongly hydrophobic, quite long segmented wormlike micelles are obtained, which had not been found in previously investigated diblock and linear ABC triblock copolymers solution. Additionally, raspberry micelles with beads dispersed on the core also occur in the strong segregation regime of bulk star ABC triblock copolymers. Furthermore, the aggregate morphology of ABC star triblock copolymers is strongly influenced by the addition of linear AB diblock copolymers. The most significant feature is that the long segmented worms will become shorter, to form hamburger micelles with the addition of AB diblock copolymers. These simulations are in good agreement with the experimental findings by Lodge's group.

Introduction

Due to the potential application in areas such as microreactors, biological function, and drug delivery, much attention has been focused on investigating the self-assembling behavior of amphiphilic block copolymers in solution both experimentally and theoretically. Block copolymers can self-assemble in solution into various structures, such as spherical micelles, rods, bilayers (lamellae and vesicles), tubules, large compound micelles (LCMs), and hexagonally packed hollow hoops.[1] Eisenberg and co-workers have pioneered the field of micellar morphology control with the so-called "crew-cut" micelles.[1] In the past few years, the self-assembly of AB diblock and ABA triblock copolymers in solution has been well and widely investigated.[1−3] Due to the developments in the field of polymer synthesis, investigations have begun on the effects of polymer architecture on the self-assembled morphology of complex macromolecules. In particular, it was recently demonstrated that amphiphilic block copolymers containing more than one hydrophobic block which are incompatible to each other can self-assemble in solution into subdivided multicompartment structures. The concept of multicompartment micelles was originally inspired by biological systems in which a single eukaryotic cell, comprising many different subunits, can perform an array of distinct functions.[4] Similarly for amphiphilic block copolymers, the micellar corona could be composed of biocompatible materials labeled with selective recognition elements for targeting drug or gene delivery, and the micellar core subdivided into several compartments could in turn provide distinct chemical environments to store various drug molecules, such as gene therapy agents, or pesticides, etc.[5]

Recently, to obtain multicompartment micelles, linear multiblock copolymer with two hydrophobic block have been widely investigated, including the linear ABC triblock[6−14] and ABCA tetrablock copolymers.[15] In general, however, the above-mentioned micellar structures feature a concentric arrangement of core-shell-corona domains regardless of the overall micelle shape, due to the sequential linkage of the different blocks.[4] Very recently, star ABC triblock copolymers in dilute aqueous solution were studied experimentally by Li et al.[4,16,17] They first observed the self-assembled multicompartment structure such as segmented wormlike micelles formed by ABC star terpolymers with two incompatible hydrophobic blocks in solution. For ABC star terpolymers, in contrast, the mandatory convergence of the three immiscible blocks at one common junction point suppresses the formation of concentric structures and leads to an array of new morphologies with compartmentalized micellar cores.[4] In particular, control over the shape and size of the aggregates is of fundamental importance to obtain nanoscopic multicompartment micelles. Furthermore, blending block copolymers offers a promising and economic solution to this problem. It has been demonstrated that uniform morphologies[18,19] and target size[20−22] can be achieved through suitable blending conditions. Unfortunately, it is not easy to experimentally investigate this kind of complex system systematically. In this regard, computer simulations offer an efficient and expedient way of investigating the complex aggregate structure. This article describes our simulation results obtained using this strategy.

Various theoretical methods have been used to investigate polymer micellar morphologies including dynamic density

* Address correspondence to this author. E-mail: pingtang@fudan.edu.cn (P.T.), yuliangyang@fudan.edu.cn (Y.L.Y.).

10.1021/jp067650v CCC: $37.00
Published on Web 02/01/2007

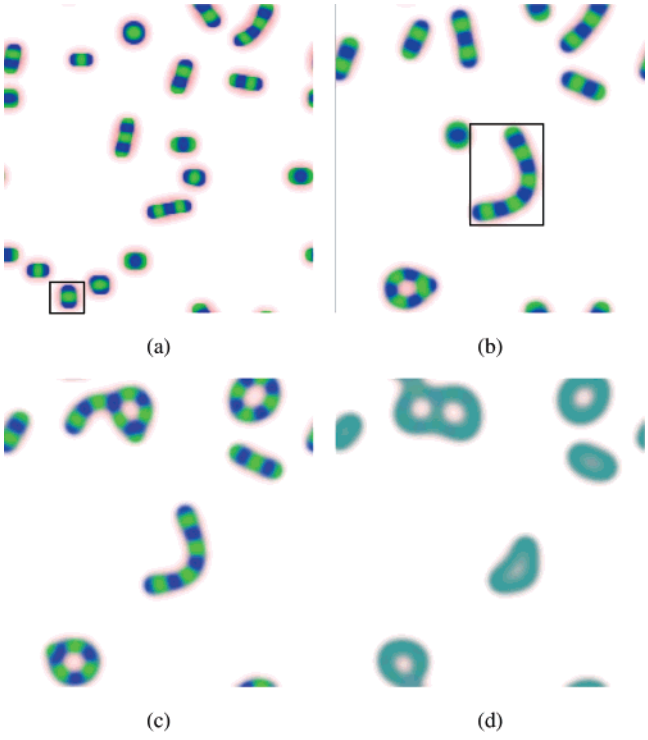

Figure 1. Morphologies of amphiphilic ABC star triblock copolymer in dilute solution with $\chi\bar{N} = 22$, $\chi_{AS}\bar{N} = -5$, and $\chi_{BS}\bar{N} = \chi_{CS}\bar{N} = 45$: A (red), B (green), C (blue), and solvent (white). (a) Star ABC(5-6-6), a hamburger micelle, is denoted in the pane; (b) star ABC(5-10-10), a segmented worm like micelle, is denoted in the pane; (c) star ABC-(5-12-12); (d) star ABC(5-14-14).

functional theory (DDFT),[23−25] Monte Carlo simulation,[26,27] Brownian dynamics simulations,[28] and dissipative particle dynamics.[29] Recently, the real-space direct implementation of SCFT in bulk proposed by Drolet and Fredrickson[30−32] was extended to deal with the self-assembling behavior of block copolymers in solution by Liang's group[33,34] and our group, where this method was used to investigate linear ABC triblock copolymers and diblock copolymer blends with different chain length in solution.[35,36]

In this paper, 2D real space self-consistent field theory is used to conduct ABC star triblock copolymer and blends with their counterpart AB diblock copolymers in solution. This work is an extension of our previous work cited in the preceding.[35,36] By investigating the relative length of hydrophilic and hydrophobic blocks, some specific multicompartment structures including long segmented wormlike, toroidal segmented, and raspberrylike micelles are obtained. Moreover, the introduction of AB diblock copolymers strongly influences the self-assembled morphologies of star ABC triblock copolymers.

Theoretical Method

Consider a mixture of n_{p1} star ABC triblock copolymers with their counterpart n_{p2} AB diblock copolymers self-assembled in n_S solvent molecules in our simulation. Each star ABC triblock copolymer chain contains $N_1 = N_{A1} + N_{B1} + N_C$ and each AB diblock copolymer contains $N_2 = N_{A2} + N_{B2}$ segments. For simplicity, we assume that the diblock copolymers have the same A and B block length with ABC triblock copolymers and the two blended polymers have the same number of chains, i.e., $N_{A2} = N_{A1}$, $N_{B2} = N_{B1}$, and $n_{p1} = n_{p2}$. The number-average chain length of the polymer blend, $\bar{N} = (N_{A1} + N_{B1} + N_C + N_{A2} + N_{B2})/2$, is used as the reference chain length. For the star ABC triblock copolymer, the reference chain length is $\bar{N} = N_1$. Accordingly, the composition (average volume fractions) of species of triblock and diblock copolymers in the blend is $f_{A1} = N_{A1}/2\bar{N}$ and $f_{A2} = N_{A2}/2\bar{N}$, respectively. The composition of species B and C in triblock and diblock copolymers is $f_{B1} = N_{B1}/2\bar{N}$, $f_{B2} = N_{B2}/2\bar{N}$, and $f_C = N_C/2\bar{N} = 1 - f_{A1} - f_{A2} - f_{B1} - f_{B2}$, respectively. Therefore, the volume fraction of the blend of ABC triblock and AB diblock copolymers is $f_1 = f_{A1} + f_{A2} + f_C$ and $f_2 = 1 - f_1$, respectively. The total concentration of the polymer in solution is set as f_p and thus the solvent concentration is $f_S = 1 - f_P$. The copolymer is assumed to be incompressible, with each polymer segment taking the same volume ρ_0^{-1} and each solvent molecule taking the same volume, i.e., $v_S = \rho_0^{-1}$. Thus the total volume of the solution system is $V = (n_{p1}N_1 + n_{p2}N_2)/\rho_0 + n_S v_S$. The segment−segment interaction or the segment−solvent interaction is represented by Flory−Huggins interaction parameter $\chi_{KK'}$, where $\chi_{KK'}$ represents the interaction between K and K′ segments (with K or K′ for species A, B, C, or S, respectively). In the SCFT, a mean field w_K represents the total interaction experienced by a segment K conjugates to the segment density field ϕ_K. Similarly, solvent molecules are considered to be in a field of w_S conjugates to the solvent density field ϕ_S. Hence, the free energy (in units of k_BT) of the ABC star triblock copolymer blended with AB diblock copolymer in solution is given by

$$\begin{aligned} F = &- f_p f_1 \ln[Q_1/(Vf_p f_1)] - f_p f_2 \ln[Q_2/(Vf_p f_2)] - \\ &\bar{N} f_S \ln(Q_S/(f_S V)) - 1/V \int d\mathbf{r}[w_A\phi_A + w_B\phi_B + w_C\phi_C + \\ &w_S\phi_S + \xi(1 - \phi_A - \phi_B - \phi_C - \phi_S)] + \\ &1/V \int d\mathbf{r}[\chi_{AB}\bar{N}\phi_A\phi_B + \chi_{AC}\bar{N}\phi_A\phi_C + \chi_{BC}\bar{N}\phi_B\phi_C + \\ &\chi_{AS}\bar{N}\phi_A\phi_S + \chi_{BS}\bar{N}\phi_B\phi_S + \chi_{CS}\bar{N}\phi_C\phi_S] \quad (1) \end{aligned}$$

where $Q_1 = \int d\mathbf{r}\, q_K(\mathbf{r},N_K)$ ($N_K = N_{A1}, N_{B1}, N_C$) and $Q_2 = \int d\mathbf{r}\, q(\mathbf{r},N_2)$ are the partition function of a single chain of ABC star triblock and AB diblock copolymers, respectively. And $Q_S = \int d\mathbf{r} \exp(-w_S(\mathbf{r})/\bar{N})$ is the partition function of the solvent in the effective chemical potential field w_S. $q(\mathbf{r},s)$ is the end segment distribution function representing the probability for a chain of $s + 1$ beads to have its end at position $\mathbf{r}$ which satisfies a modified diffusion equation using a flexible Gaussian chain model:

$$\frac{\partial}{\partial s} q(\mathbf{r},s) = \frac{\bar{N}a^2}{6}\nabla^2 q(\mathbf{r},s) - w_K q(\mathbf{r},s) \quad (2)$$

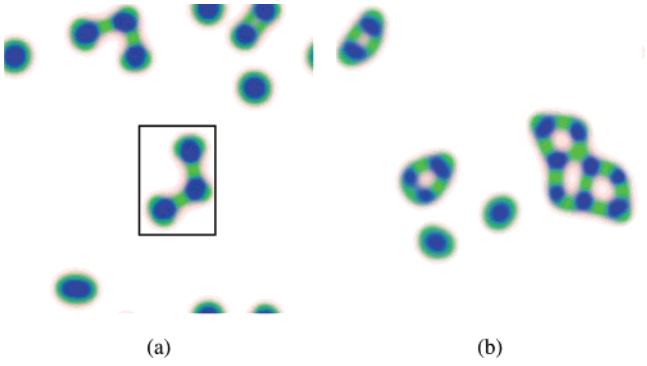

Figure 2. Morphologies of amphiphilic ABC star triblock copolymer in dilute solution with $\chi\bar{N} = 22$, $\chi_{AS}\bar{N} = -5$, and $\chi_{BS}\bar{N} = \chi_{CS}\bar{N} = 45$: A (red), B (green), C (blue), and solvent (white). (a) Star ABC(5−10-14), a bead-on-string micelle, is denoted in the pane and (b) star ABC-(5-12-14).

where $s \in [0,N_K]$ is a contour parameter that parametrizes each segment from core $s = 0$ to the outer end $s = N_{A1}$, N_{B1}, N_C for star ABC triblock copolymers, while for AB diblock copolymers from $s = 0$ to N_2 along the AB chain. The initial condition is $q_K(\mathbf{r},0) = q_L^+(\mathbf{r},0)q_M^+(\mathbf{r},0)$, where (K L M) $\in$ {(A B C),-(B C A),(C A B)}(K L M) for star ABC triblock copolymers[37] and $q(\mathbf{r},0) = 1$ for AB diblock copolymers, respectively. Because the two ends of the block copolymer are different, a second distribution function $q^+(\mathbf{r},s)$ is needed, which also satisfies eq 2 but with the right-hand side multiplied by -1 and the initial condition is $q^+(\mathbf{r},N_K) = 1$ (K = N_{A1}, N_{B1}, N_C) for star ABC triblock and $q^+(\mathbf{r},N_2) = 1$ for AB diblock copolymers. Minimizing the free energy in eq 1 with respect to density and pressure leads to the following self-consistent field equations at the equilibrium:[38]

$$\phi_A(\mathbf{r}) = f_p V\left[\frac{1}{2Q_1\bar{N}}\int_0^{N_{A1}} ds q(\mathbf{r},s)\, q^+(\mathbf{r},s) + \frac{1}{2Q_2\bar{N}}\int_0^{N_{A2}} ds q(\mathbf{r},s)\, q^+(\mathbf{r},s)\right] \quad (3)$$

$$\phi_B(\mathbf{r}) = f_p V\left[\frac{1}{2Q_1\bar{N}}\int_0^{N_{B1}} ds q(\mathbf{r},s)\, q^+(\mathbf{r},s) + \frac{1}{2Q_2\bar{N}}\int_{N_{A2}}^{N_{A2}+N_{B2}} ds q(\mathbf{r},s)\, q^+(\mathbf{r},s)\right] \quad (4)$$

$$\phi_C(\mathbf{r}) = \frac{f_p V}{2Q_1\bar{N}}\int_0^{N_C} ds q(\mathbf{r},s)\, q^+(\mathbf{r},s) \quad (5)$$

$$\phi_S(\mathbf{r}) = \frac{\exp(-\omega_S(r)/\bar{N})}{Q_S} \quad (6)$$

$$\omega_A(\mathbf{r}) = \chi_{AB}\bar{N}\phi_B(\mathbf{r}) + \chi_{AC}\bar{N}\phi_C(\mathbf{r}) + \chi_{AS}\bar{N}\phi_S(\mathbf{r}) + \xi(\mathbf{r}) \quad (7)$$

$$\omega_B(\mathbf{r}) = \chi_{AB}\bar{N}\phi_A(\mathbf{r}) + \chi_{BC}\bar{N}\phi_C(\mathbf{r}) + \chi_{BS}\bar{N}\phi_S(\mathbf{r}) + \xi(\mathbf{r}) \quad (8)$$

$$\omega_C(\mathbf{r}) = \chi_{AC}\bar{N}\phi_A(\mathbf{r}) + \chi_{BC}\bar{N}\phi_B(\mathbf{r}) + \chi_{CS}\bar{N}\phi_S(\mathbf{r}) + \xi(\mathbf{r}) \quad (9)$$

$$\phi_A(\mathbf{r}) + \phi_B(\mathbf{r}) + \phi_C(\mathbf{r}) + \phi_S(\mathbf{r}) = 1 \quad (10)$$

Equations 3−10 can be solved numerically in real space by using the combinatorial screening algorithm proposed by Drolet and Fredrickson.[30,31] The algorithm consists of randomly generating the initial values of the fields $\omega_K(\mathbf{r})$. By using an alternating-direct implicit (ADI) method the diffusion equations are then integrated to obtain $q(\mathbf{r},s)$ and $q^+(\mathbf{r},s)$. Next, the right-hand sides of eqs 3−6 are evaluated to obtain new values for the volume fractions of blocks A, B, C and solvent S. The simulation is carried out until the phase patterns are stable and the free energy difference between two iterations is smaller than 10^{-5}, i.e., $\Delta F < 10^{-5}$. It is noted that the resulting aggregates are found to be strongly influenced by the initial fluctuation amplitude, possibly corresponding to different experimental preparation conditions, such as the concentration and quenching temperature. As a result, our simulations are performed using the same initial fluctuation amplitude value on the order of 10^{-4} with random uniform distribution to ensure that these obtained different morphologies are not influenced by the initial condition. Furthermore, the simulation was repeated at least 10 times with different random states and random-number generator seeds to guarantee the structures are not observed on occasion. For simplicity, the simulations are carried out on the two-dimensional space of a 200 × 200 square lattice with periodic boundary conditions applied. The grid size is set to be $\Delta x = 0.35$.

Results and Discussion

Hereafter, we use "star ABC(N_{A1}-N_{B1}-N_C)" and "diblock AB-(N_{A2}-N_{B2})" to represent the star triblock copolymers and the diblock copolymers containing the block lengths indicated in the brackets, respectively. The total polymer concentration is set to be $f_p = 0.1$. Compared to the ABC linear triblock copolymer melts, an additional entropic effect arises due to the junction constraint of center cores in star ABC and thus the parameter space of ABC star triblock copolymer in solution is even larger. To emphasize the strong topological constraint that regulates the geometry of the microphases formed by star ABC triblock copolymers and also to obtain multicompartment aggregates, in this article, all three block species are mutually effective repulsive so that A, B, and C blocks segregate into distinct nanodomains, a necessary condition to promote the formation of multicompartment aggregates. For the sake of simplicity, we assume symmetric interactions between different blocks, i.e., $\chi_{AB}\bar{N} = \chi_{BC}\bar{N} = \chi_{AC}\bar{N} = \chi\bar{N}$. Moreover, block A is assumed to be hydrophilic and $\chi_{AS}\bar{N}$ is fixed to be $\chi_{AS}\bar{N} = -5$, and the other two blocks B and C are hydrophobic with variable parameters $\chi_{BS}\bar{N}$ and $\chi_{CS}\bar{N}$. The A block length is set to be $N_{A1} = N_{A2} = 5$ throughout our simulations, a suitable value chosen by our calculation tests that assures the aggregates exist and there is no precipitation. In the following illustrations, four different colors, i.e., red, green, blue, and white, are assigned to A, B, C species and the solvent, respectively. To investigate the aggregation behavior of the blends of star ABC triblock and AB diblock copolymers in solution, the self-assembly of amphiphilic star ABC triblock copolymers in solution is first conducted.

A. ABC Star Triblock Copolymer in Solution. We focus on the effect of the relative hydrophobic block length on the aggregate structure under symmetric or asymmetric interaction of B and C species to solvent. Therefore, the ABC star triblock copolymer we study can be placed into two categories in terms of hydrophobicity degree of blocks B and C, i.e., $\chi_{BS}\bar{N} = \chi_{CS}\bar{N}$ and $\chi_{BS}\bar{N} \neq \chi_{CS}\bar{N}$, respectively.

1. Equal hydrophobicity of Blocks B and C ($\chi_{BS}\bar{N} = \chi_{CS}\bar{N}$). We first choose medium segregation degree for different blocks ($\chi\bar{N} = 22$ and $\chi_{BS}\bar{N} = \chi_{CS}\bar{N} = 45$), i.e., the equal hydrophobicity of blocks B and C; the self-assembled morphologies are shown in Figure 1 by increasing the length of hydrophobic blocks B and C simultaneously. Due to the topological characteristics of ABC star copolymer in which three immiscible blocks must converge at a junction point, the concentric structure often found in linear ABC triblock copolymer solution is suppressed and multicompartmentalized micellar cores occur instead. With increasing the hydrophobic block length, the morphologies change from hamburgers (the B block forming hamburger with C block as the buns on the top and bottom sides, as shown in Figure 1a in the pane) to segmented worms to vesicles, which is qualitatively in agreement with the experimental observations.[4] Actually, This transition is quite similar to the spheres-to-cylinders-to-vesicles transition reported in diblock copolymers with increasing the hydrophobic block length. The morphologies of hamburgers, along with short segmented worm-like micelles and long segmented worm-like micelles, are observed by star ABC(5-6-6) and star ABC(5-10-10) in Figure 1, parts a and b, respectively. Segmented worm-like micelles were first found in a water-soluble poly(ethylene oxide), polyethylethylene, and

poly(perfluoropropylene) star triblock copolymer system by Li et al.[17] These micelles are the previously unreported so-called multicompartment micelles, where the core is constructed by microphase-segregated blocks B and C with alternating B and C layers due to the immiscibility between blocks B and C and the nearly equal length of blocks B and C. When the ratio of hydrophobic to hydrophilic block length is large enough, relatively long segmented wormlike micelles occur due to the self-attraction of humberger micelles. From the notation of Li et al.,[17] this is because many lamellar cores are able to share the quite short hydrophilic blocks to screen hydrophobic cores. As the fraction of hydrophobic blocks B and C is increased, an interesting morphology, i.e., the toroidal or ringlike segmented micelle, is observed in Figure 1c. We should note that it is difficult to delineate the difference between the ringlike segmented micelle and vesicle with lamellar wall in our 2D calculations. However, we can deduce that this structure should be the ringlike segmented micelle according to its evolution from segmented wormlike micelles. The formation of the ringlike micelle appears to result from the high energy of end caps of segmented worms.[39] Recently, uniform toroidal micelles were first found in charged amphiphilic linear ABC triblock copolymer dilute solution due to the charge interactions leading to self-attraction of cylinders.[40] Further increasing B and C block fraction leads to the formation of vesicles shown in Figure 1d. Vesicles formed by star triblock copolymers were also found by Li et al.[4] However, the observed vesicle here forms the three-layer A-(B+C)-A structure in contrast to the A-B-A three-layer vesicle in AB diblock copolymers and the A-B-C-B-A five-layer vesicle in ABC linear triblock copolymers.[15,36] As the interaction between polymers is not quite strong, species B and C are partially miscible and placed in the vesicle wall. Actually, due to one more hydrophobic block and the topological constraint in ABC star triblock copolymers, the parameter space for finding vesicles in star ABC triblock copolymers solution is very limited. First, the hydrophobic block length is much longer than that of the hydrophilic block, as in the case of AB diblock copolymers, i.e., the diblock copolymer usually forms the so-called crew-cut aggregates. Second, the hydrophobicity of blocks B and C should be large enough. Finally, the hydrophobicity degree of blocks B and C should be comparable, i.e., $\chi_{BS}N_B \approx \chi_{CS}N_C$. For this reason, observations of vesicles in most experiments have been scarce in a wide range of block lengths even for corona blocks considerably shorter than the core block in star ABC triblock copolymer solution.

Examples of the aggregate morphology for cases with unequal lengths of the hydrophobic blocks B and C ($N_B \neq N_C$) are shown in Figure 2, for varying relative lengths of blocks B and C. Figure 1b shows the results obtained with an increase in C block length while B block length is fixed, say star(5-10-14), showing that short wormlike micelles are found, here referred to as bead-on-string worm; these are somewhat different from the above-mentioned segmented lamellar wormlike micelles. To our knowledge, the specific micelle with longer C block forming the inner core capped by the shorter B block forming the outer shell and connected by a slim neck is observed for the first time in our simulation. The formation of different structures such as hamburger, core-shell-corona, bead-on-string, and long segmented wormlike micelles result mainly from balancing interfacial energy between the core and solvent. The interfacial energy can be calculated as $F_{interface} = \gamma s$, with $\gamma = (kT/a^2)(\chi_{core-solvent}/6)^{0.5}$, where γ is the surface tension, s is the interfacial area per chain, a is the monomer length.[41,42] When the $F_{interface}$ between the blocks B-solvent and C-solvent is comparable (as the result of close block length and hydrophobicity of B and C blocks), layer-by-layer structures are favorable. However, when the two $F_{interface}$ have large differences, the species with a small value will tend to cover the other component to screen it from the solvent. As a result, if the $F_{interface}$ between one block and solvent is much larger than that for another block, only core-shell-corona structures can be observed. The result of increasing N_C from 12 to 14, with the B block length fixed at $N_B = 12$, may be seen by comparison of Figures 1c and 2b, respectively, showing that complex network and ringlike segmented micelles are obtained due to the self-attraction of segmented worm micelles. The C core only becomes larger (not shown here) with further increasing N_C for fixed B block lengths of 10 or 12. For $N_B = 6$ and $N_B = 14$, with increase of the C block length, only core-shell-corona and large compound micelles are obtained (not shown here). Since the blocks B and C are topologically symmetric, similar results are expected on increasing the B block length with density distribution exchanged between B and C species.

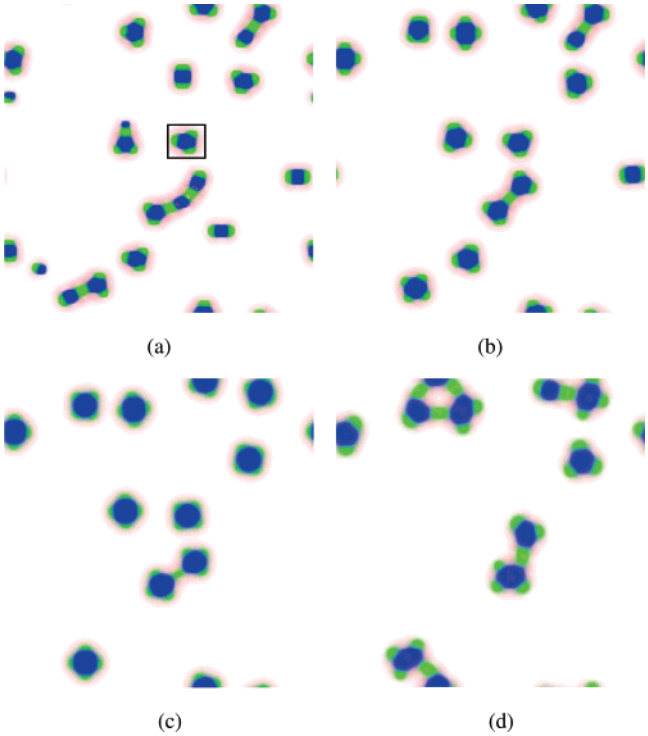

Figure 3. Morphologies of amphiphilic ABC star triblock copolymer in dilute solution with $\chi\bar{N} = 35$, $\chi_{AS}\bar{N} = -5$, and $\chi_{BS}\bar{N} = \chi_{CS}\bar{N} = 45$: A (red), B (green), C (blue), and solvent (white). (a) Star ABC(5-6-8), a raspberry micelle, is denoted in the pane; (b) star ABC(5-6-10); (c) star ABC(5-6-14); and (d) star ABC(5-10-14).

Moreover, at strong segregation degree, e.g., $\chi\bar{N} = 35$, Figure 3 shows some interesting morphologies with unequal block length of B and C. For star ABC(5-6-8) in Figure 3a, a type of micelles (in the pane) with three small semicircular B beads dispersed on a large C core appear corresponding to raspberry-like micelles in 3D. Raspberry-like micelles have been observed in linear triblock copolymer bulk at first[43−45] and later in aqueous[4,46] both by experiments and simulations.[47] The similar structure is also predicted earlier by Dormidontova and Khokhlov[6] for linear ABC triblock terpolymers in strong and superstrong segregation limit. Our simulation results are qualitatively consistent with the experimental results and predictions that raspberry micelles only occur at the strong segregation regime of copolymers. In the strong segregation regime of block copolymers, the short block by forming beads is dispersed

Figure 4. Morphologies of star ABC(3-9-9) in dilute solution with $\chi\bar{N} = 40$, $\chi_{AS}\bar{N} = -5$, and $\chi_{BS}\bar{N} = \chi_{CS}\bar{N} = 40$: A (red), B (green), C (blue), and solvent (white).

outside the long block forming core to decrease the interfacial energy between strong segregation blocks. In Figure 3b for star ABC(5-6-10), with increasing the difference between the B and C block length, segmented worm structures almost disappeared and the core of C species becomes bigger with smaller beads distributed on it. With further increase of C block length for star ABC(5-6-14) in Figure 3c, only raspberry micelles are observed with dispersed smaller beads. However, with simultaneously increasing the B and C block lengths, as shown in Figure 3d, the beads on raspberry micelles tend to be self-attraction to form a network structure.

We should note that when we increase the microphase-segregation degree of different block species, such as $\chi N = 40$, the quite long wormlike micelles can be obtained as shown in Figure 4. Furthermore, in this case, the wormlike core is constructed by the alternating hydrophobic blocks B and C forming beads to decrease interfacial energy between blocks B and C.

2. Unequal Hydrophobicity of Blocks B and C ($\chi_{BS}\bar{N} \neq \chi_{CS}\bar{N}$). Similar to subsection 1, we set the polymer interaction $\chi\bar{N} = 22$. Due to the topological equivalence of two hydrophobic blocks of the star ABC triblock copolymer, we assume the C block is most hydrophobic ($\chi_{CS}\bar{N} = 45$) and $\chi_{BS}\bar{N} = 35$ to make the two hydrophobic blocks be chemically different. Figure 5 shows the results of increasing B block length with fixed C block length, e.g., $N_C = 10$, morphology changes from segmented bead-on-string worms to segmented worms along with toroidal segmented micelles and finally to vesicles. In Figure 5a bead-on-string worms are again observed, while segmented wormlike micelles with layer-by-layer arrangement occur in Figure 1b by star(5-10-10). Segmented wormlike micelles are obtained in Figure 5b by star(5-12-10) with symmetric hydrophobicity of blocks B and C. This phenomenon, which has been documented in the above discussions, results from balancing interfacial energy between the core and solvent. With further increase of B block length, vesicles are found by star ABC(5-17-10) in Figure 5c. This trend is similar to the results of Li et al.:[4] vesicles are formed when the composition of the less hydrophobic block is more than that of the most hydrophobic block.

B. ABC Star Triblock Copolymer Blended with AB Diblock Copolymer in Solution. In this section, we investigate the self-assembled structure of star ABC triblock corpolymers blended with AB diblock copolymers in solution. To reduce the large parameter spaces, the A and B block lengths of diblock copolymers are set to be the same as the corresponding block lengths of the triblock copolymer, i.e., $N_{A1} = N_{A2}$ and $N_{B1} = N_{B2}$. The A block length is also fixed to be $N_{A1} = N_{A2} = 5$, thus the aggregate behavior formed by block copolymer blends is investigated by varying the length of blocks B and C. We further assume triblock terpolymers and diblock copolymers are mixing with the same number of molecules, i.e., $n_{p1} = n_{p2}$, and the total polymer concentration remains $f_p = f_1 + f_2 = 0.1$, the same as the star ABC triblock copolymer solution as discussed above. Following the above discussions, two cases are considered in terms of equal hydrophobicity of blocks B and C ($\chi_{BS}\bar{N} = \chi_{CS}\bar{N}$) and unequal hydrophobicity of blocks B and C ($\chi_{BS}\bar{N} \neq \chi_{CS}\bar{N}$).

1. Equal Hydrophobicity of Blocks B and C ($\chi_{BS}\bar{N} = \chi_{CS}\bar{N}$). At first, we assume the symmetric hydrophobicity of blocks B and C, i.e., $\chi_{BS}\bar{N} = \chi_{CS}\bar{N} = 45$. The simulation results can be classified into two cases in terms of the hydrophobic block length of ABC star triblock copolymers, i.e., $N_{B1} = N_C$ and $N_{B1} \neq N_C$. When $N_{B1} = N_C$, as shown in Figure 6a for star ABC(5-10-10)/diblock AB(5-10), the self-assembled morphology changes from long segmented wormlike micelles in pure star ABC triblock copolymers (Figure 1b) into relatively short segmented wormlike micelles and hamburger micelles in blends. The addition of amphiphilic AB diblock copolymer is equivalent to the increase of hydrophilic A composition that can provide more chances to screen the hydrophobic blocks from solvent, and thus can prevent the further aggregation from forming long wormlike micelles. The very recent experimental work done by Li et al.[18] described similar results, in which the long segmented worm became uniform widened hamburger micelles by the introduction of AB diblock copolymer. When $N_{B1} < N_C$, as shown in Figure 6b−d, raspberry micelles appear again. From Figure 6b to 6d with increasing C block length, the core will become bigger with smaller beads, which is similar to raspberry micelles formed by bulk star ABC triblock copolymers (Figure 3a−c). Moreover, it is clearly seen from the concentration distribution in Figure 8a (in the middle column) that the AB diblock copolymer constructs the outer part of the beads. It

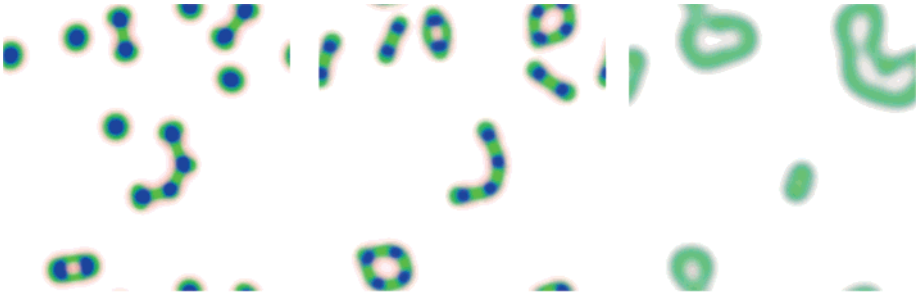

(a) (b) (c)

Figure 5. Morphologies of amphiphilic ABC star triblock copolymer in dilute solution with $\chi\bar{N} = 22$, $\chi_{BS}\bar{N} = 35$, and $\chi_{CS}\bar{N} = 45$: A (red), B (green), C (blue), and solvent (white). (a) Star ABC(5-10-10), (b) star ABC(5−12-10), and (c) star ABC(5-17-10).

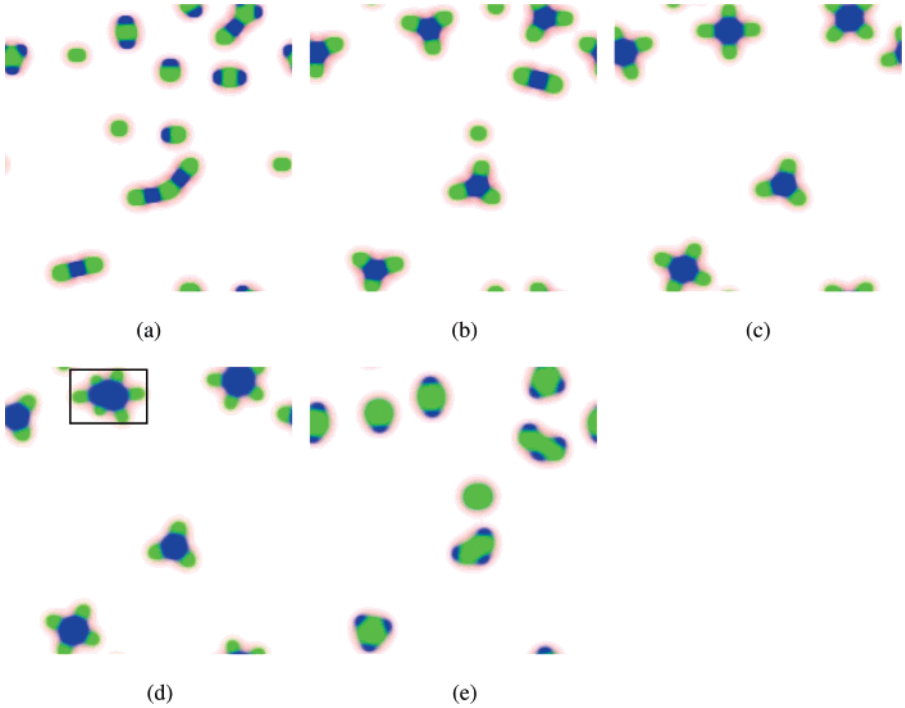

Figure 6. Morphologies of amphiphilic ABC star triblock terpolymer blended with AB diblock copolymer in dilute solution with $\chi_{BS}\bar{N} = \chi_{CS}\bar{N} = 45$: A (red), B (green), C (blue), and solvent (white). (a) Star ABC(5-10-10)/diblock AB(5-10); (b) star ABC(5-10-12)/diblock AB(5-10); (c) star ABC(5-10-17)/diblock AB(5-10); (d) star ABC(5-10-21)/diblock AB(5-10), a huge raspberry micelle is denoted in the pane and its concentration destribution is shown in Figure 8a; and (e) star ABC(5-15-10)/diblock AB(5-15).

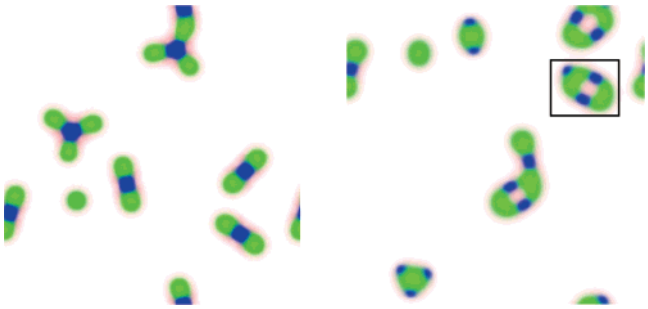

Figure 7. Morphologies of amphiphilic star ABC triblock copolymer blended with AB diblock copolymer in dilute solution with $\chi_{BS}\bar{N} = 35$ and $\chi_{CS}\bar{N} = 45$: A (red), B (green), C (blue), and solvent (white). (a) Star ABC(5-12-10)/diblock AB(5-12); (b) star ABC(5-15-10)/diblock AB(5-15), a new elliptical micelle is denoted in the pane and its concentration distribution is shown in Figure 8b.

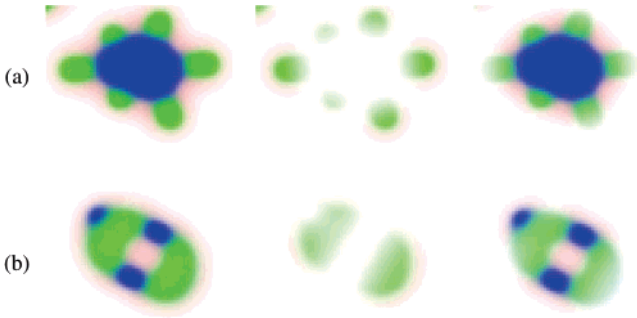

Figure 8. Concentration distributions of star ABC triblock terpolymers blend diblock AB copolymers: A (red), B (green), C (blue), and solvent (white). (a) Raspberry micelle in Figure 6d (in the pane); (b) cyclic micelle in Figure 7b (in the pane). From left to right, the columns represent concentration distributions of the micelle formed by star ABC and AB diblock copolymers, diblock AB, and star ABC triblock copolymers, respectively.

should be noted that even if the total quantity of the B block is larger than that of the C block, i.e., $N_B = (N_{B1} + N_{B2}) \geq N_C$, the C block of the star ABC triblock copolymer will form the inner core with the dispersed B block forming the outer core (beads). When $N_{B1} > N_C$, similar raspberry micelles are again obtained as shown in Figure 6e for the star ABC(5-15-10)/diblock AB(5-15), but the inner core is formed by the B block with quite small C beads distributed outside.

2. Unequal Hydrophobicity of Blocks B and C ($\chi_{BS}\bar{N} \neq \chi_{CS}\bar{N}$). Then we consider the case of asymmetric hydrophobicity of blocks B and C, e.g., $\chi_{BS}\bar{N} = 35$and $\chi_{CS}\bar{N} = 45$. As the C block is more hydrophobic than the B block, the C block will form the inner core to minimize unfavorable contact with the solvent. Accordingly, raspberry micelles are usually found for $N_{B1} \leq N_C$. When$N_{B1} > N_C$, Figure 7a shows the morphologies of star ABC(5-12-10)/diblock AB(5-12). Compared to the case of equal hydrophobicity of blocks B and C (Figure 5b), long segmented worm micelles disappear and uniform hamburger micelles are obtained instead. Specifically, a new elliptical structure by star ABC(5-15-10)/diblock AB(5-15) in Figure 7b is observed. From the density distribution shown in the middle column of Figure 8b, the diblock AB(5-15) is located rather far from the center and constructs most of the two ends of the long axis of the elliptical structure. Furthermore, we should note that this elliptical structure does not occur for the case of $\chi_{BS}\bar{N} = \chi_{CS}\bar{N}$.

Summary

We have interpreted the self-assembled morphologies of amphiphilic ABC star triblock copolymers and the blends with their corresponding AB diblock copolymers in solution by using 2D real-space implementation of self-consistent field theory. To obtain multicompartment micelles formed by complex topological copolymers, the A block is assumed as hydrophilic and B and C blocks are hydrophobic, leading to the microphase-segregated hydrophobic BC core. The hydrophilic block length is further fixed to be $N_A = 5$, and thus the self-assembly of block copolymers is investigated systematically by tuning the

relative length of hydrophobic blocks B and C under the condition of equal and unequal hydrophobicity between blocks B and C, respectively.

For symmetric hydrophobicity of blocks B and C, the micellar structure follows the sequence from hamburger, to segmented wormlike micelles, and finally to vesicles with increasing hydrophobic block lengths of B and C simultaneously. This transition is quite similar to the spheres-to-cylinders-to-vesicles transition reported in diblock copolymers with increasing the hydrophobic block length. The condition of segmented worm formation requires that the interface energy ($F_{\text{interface}}$) between B-solvent and C-solvent should be comparable and the ratio of hydrophobic to hydrophilic length should be so large that the hamburger must stack together to share the limited length of the hydrophilic block to screen the solvent efficiently. Otherwise, when the interface energy between B-solvent and C-solvent becomes unequal, the specific bead-on-string micelles are found because the block with less $F_{\text{interface}}$ will tend to cover the higher $F_{\text{interface}}$ block to screen from the solvent. In addition, relatively long segmented wormlike micelles and raspberry micelles can be found in the strong segregation regime of bulk star triblock copolymers.

Furthermore, the aggregate morphology of ABC star triblock copolymers is strongly influenced by the addition of linear AB diblock copolymers. The significant feature is that the long segmented wormlike micelles occurring in star ABC triblock copolymer solution will change to be the shorter segmented worms or hamburger micelles. When the hydrophobic block length becomes asymmetric, i.e., $N_B \neq N_C$, raspberry micelles are usually observed. Specifically, an interesting elliptical micelle is found only when the hydrophobicity of blocks B and C is asymmetric and the B block length is much longer than that of the C block.

These findings and speculations provide guidance to designing multicompartment aggregated structure from complex topological multiblock copolymer solution.

Acknowledgment. We thank the National Basic Research Program of China (Grant No. 2005CB623800) and the Excellent Research Group of NSF of China for financial support financial support . The NSF of China (Grant Nos. 20234010, 20474012, 20674012, and 20574015) is also acknowledged.

References and Notes

(1) Gohy, J. F. *Adv. Polym. Sci.* **2005**, *190*, 65−136.
(2) Hamley, I. W. *The Physics of Block Copolymers*; Oxford University Press: New York 1998.
(3) Riess, G. *Prog. Polym. Sci.* **2003**, *28*, 1107.
(4) Li, Z.; Hillmyer, M. A.; Lodge, T. P. *Langmuir* **2006**, *22*, 9409−9417.
(5) Lodge, T. P.; Rasdal, A.; Li, Z. B.; Hillmyer, M. A. *J. Am. Chem. Soc.* **2005**, *127*, 17608−17609.
(6) Dormidontova, E. E.; Khokhlov, A. R. *Macromolecules* **1997**, *30*, 1980−1991.
(7) Kriz, J.; Masar, B.; Plestil, J.; Tuzar, Z.; Pospisil, H.; Doskocilova, D. *Macromolecules* **1998**, *31*, 41−51.
(8) Liu, S. Y.; Armes, S. P. *J. Am. Chem. Soc.* **2001**, *123*, 9910−9911.
(9) Gohy, J. F.; Willet, N.; Varshney, S.; Zhang, J. X.; Jerome, R. *Angew. Chem., Int. Ed.* **2001**, *40*, 3214.
(10) Bieringer, R.; Abetz, V.; Muller, A. H. E. *Eur. Phys. J. E* **2001**, *5*, 5−12.
(11) Butun, V.; Wang, X. S.; Banez, M. V. D.; Robinson, K. L.; Billingham, N. C.; Armes, S. P.; Tuzar, Z. *Macromolecules* **2000**, *33*, 1−3.
(12) Patrickios, C. S.; Lowe, A. B.; Armes, S. P.; Billingham, N. C. *J. Polym. Sci., Part A*: *Polym. Chem.* **1998**, *36*, 617−631.
(13) Sfika, V.; Tsitsilianis, C.; Kiriy, A.; Gorodyska, G.; Stamm, M. *Macromolecules* **2004**, *37*, 9551−9560.
(14) Kubowicz, S.; Baussard, J. F.; Lutz, J. F.; Thunemann, A. F.; von Berlepsch, H.; Laschewsky, A. *Angew. Chem., Int. Ed.* **2005**, *44*, 5262−5265.
(15) Brannan, A. K.; Bates, F. S. *Macromolecules* **2004**, *37*, 8816−8819.
(16) Li, Z. B.; Hillmyer, M. A.; Lodge, T. P. *Nano Lett.* **2006**, *6*, 1245−1249.
(17) Li, Z. B.; Kesselman, E.; Talmon, Y.; Hillmyer, M. A.; Lodge, T. P. *Science* **2004**, *306*, 98−101.
(18) Li, Z. B.; Hillmyer, M. A.; Lodge, T. P. *Macromolecules* **2006**, *39*, 765−771.
(19) Gao, W. P.; Bai, Y.; Chen, E. Q.; Li, Z. C.; Han, B. Y.; Yang, W. T.; Zhou, Q. F. *Macromolecules* **2006**, *39*, 4894−4898.
(20) Won, Y. Y.; Brannan, A. K.; Davis, H. T.; Bates, F. S. *J. Phys. Chem. B* **2002**, *106*, 3354−3364.
(21) Jain, S.; Bates, F. S. *Macromolecules* **2004**, *37*, 1511−1523.
(22) Luo, L. B.; Eisenberg, A. *J. Am. Chem. Soc.* **2001**, *123*, 1012−1013.
(23) Guo, S. L.; Hou, T. J.; Xu, X. J. *J. Phys. Chem. B* **2002**, *106*, 11397−11403.
(24) Uneyama, T.; Doi, M. *Macromolecules* **2005**, *38*, 5817−5825.
(25) van Vlimmeren, B. A. C.; Maurits, N. M.; Zvelindovsky, A. V.; Sevink, G. J. A.; Fraaije, J. *Macromolecules* **1999**, *32*, 646−656.
(26) Dotera, T.; Hatano, A. *J. Chem. Phys.* **1996**, *105*, 8413.
(27) Ji, S. C.; Ding, J. D. *Langmuir* **2006**, *22*, 553−559.
(28) Noguchi, H.; Takasu, M. *Phys. Rev. E* **2001**, *64*, 041913.
(29) Yamamoto, S.; Maruyama, Y.; Hyodo, S. *J. Chem. Phys.* **2002**, *116*, 5842.
(30) Drolet, F.; Fredrickson, G. H. *Phys. Rev. Lett.* **1999**, *83*, 4317−4320.
(31) Drolet, F.; Fredrickson, G. H. *Macromolecules* **2001**, *34*, 5317−5324.
(32) Fredrickson, G. H.; Ganesan, V.; Drolet, F. *Macromolecules* **2002**, *35*, 16−39.
(33) He, X. H.; Liang, H. J.; Huang, L.; Pan, C. Y. *J. Phys. Chem. B* **2004**, *108*, 1731−1735.
(34) Jiang, Y.; Chen, T.; Ye, F. W.; Liang, H. J.; Shi, A. C. *Macromolecules* **2005**, *38*, 6710−6717.
(35) Li, X. A.; Tang, P.; Qiu, F.; Zhang, H. D.; Yang, Y. L. *J. Phys. Chem. B* **2006**, *110*, 2024−2030.
(36) Wang, R.; Tang, P.; Qiu, F.; Yang, Y. L. *J. Phys. Chem. B* **2005**, *109*, 17120−17127.
(37) Tang, P.; Qiu, F.; Zhang, H. D.; Yang, Y. L. *J. Phys. Chem. B* **2004**, *108*, 8434−8438.
(38) Eugene, H.; Anne Marie, S. *J. Chem. Phys.* **1975**, *62*, 1327−1331.
(39) In, M.; Aguerre-Chariol, O.; Zana, R. *J. Phys. Chem. B* **1999**, *103*, 7747−7750.
(40) Pochan, D. J.; Chen, Z. Y.; Cui, H. G.; Hales, K.; Qi, K.; Wooley, K. L. *Science* **2004**, *306*, 94−97.
(41) Eugene, H.; Yukiko, T. *J. Chem. Phys.* **1972**, *56*, 3592−3601.
(42) Bhargava, P.; Zheng, J. X.; Li, P.; Quirk, R. P.; Harris, F. W.; Cheng, S. Z. D. *Macromolecules* **2006**, *39*, 4880−4888.
(43) Breiner, U.; Krappe, U.; Jakob, T.; Abetz, V.; Stadler, R. *Polym. Bull.* **1998**, *40*, 219−226.
(44) Ritzenthaler, S.; Court, F.; David, L.; Girard-Reydet, E.; Leibler, L.; Pascault, J. P. *Macromolecules* **2002**, *35*, 6245−6254.
(45) Ritzenthaler, S.; Court, F.; Girard-Reydet, E.; Leibler, L.; Pascault, J. P. *Macromolecules* **2003**, *36*, 118−126.
(46) Laschewsky, A. *Curr. Opin. Colloid Interface Sci.* **2003**, *8*, 274−281.
(47) Xia, J.; Zhong, C. L. *Macromol. Rapid Commun.* **2006**, *27*, 1110−1114.